Available online at www.sciencedirect.com
SCIENCE DIRECT®
Journal of Catalysis 225 (2004) 7–15
JOURNAL OF CATALYSIS
www.elsevier.com/locate/jcat

Increase of Pd surface area by treatment in dioxygen

Jinyi Han,[a] Guanghui Zhu,[a] Dmitri Y. Zemlyanov,[b] and F.H. Ribeiro [a,*]

[a] *Worcester Polytechnic Institute, Department of Chemical Engineering, Worcester, MA 01609-2280, USA*
[b] *Materials and Surface Science Institute, University of Limerick, Limerick, Ireland*

Received 13 November 2003; revised 22 March 2004; accepted 24 March 2004

Available online 24 April 2004

Abstract

The surface area of Pd(111) and Pd(110) single crystals increased after oxidation in O_2 transformed them to PdO. The surface area of the oxide decreased after complete reduction in H_2. The techniques of STM, TPD, XPS, AES, and LEED were employed to study the Pd(111) and Pd(110) single-crystal surfaces after they were subjected to O_2 oxidation, methane combustion, and H_2 reduction. The surface area of the treated palladium single crystals was measured by ^{18}O isotope exchange and by direct measurements using the STM image. These two methods showed agreement within 20%. After oxidation in O_2 (100 and 150 Torr) at 600 K, the surface area for both Pd(111) and Pd(110) single crystals increased by a factor of approximately two. The effect was more pronounced on the Pd(111) surface. The oxidized surfaces were covered with 3- to 4-nm semispherical oxide agglomerates that formed a "cauliflower-like" structure 10–20 nm in size. Similar surface structures were observed after exposure of the Pd single crystals to a lean O_2 and CH_4 reaction mixture (O_2:CH_4 = 10:1). Thus, the oxidized single crystal becomes amorphous. Reduction in H_2 decreased the surface area of the preoxidized Pd(111) and Pd(110) crystals. An amorphous metallic surface was produced after H_2 reduction at 373 K, whereas a smooth surface with characteristic single-crystal features was observed after reduction at 673 K. These experiments suggest that oxidizing a Pd metal catalyst or reducing an oxidized Pd catalyst, for example, before palladium metal surface area measurement, will affect the surface area of the sample. It also shows that the increase in surface area on Pd catalysts after oxidation treatment is caused by surface roughening.

Keywords: Palladium oxidation; PdO morphology; PdO surface area measurement

1. Introduction

The turnover rate (TOR) is defined as the number of molecules reacted on an active site per unit of time [1]. It is one of the most important parameters used in quantifying the properties of a catalyst [2,3]. To calculate the TOR, it is necessary to know the number of active sites, a rarely known parameter. In practice, the total surface area is measured and the total number of sites is calculated from it by assuming a certain site density. For example, the adsorption of H_2, O_2, CO, and H_2–O_2 titration is used to measure the surface area of supported metal catalysts [1,4], but the catalyst must be in the reduced state for these techniques to work; in many cases the active catalyst is not in metallic form. Palladium, which is referred as the most active catalyst for methane combustion [5], is an example. Depending on the oxygen partial pressure and the temperature, either Pd metal or Pd oxide can be the thermodynamically stable phase. In air at atmospheric pressure, PdO is the active phase up to 1073 K [6–8]. Therefore, the oxidized samples will have to be reduced to Pd metal (usually in H_2, see, for example [9–11]) before the measurement of surface area by chemisorption. It is implicitly assumed then that the surface area does not change after PdO reduction or Pd oxidation. In general, the surface area may change during reduction. Indeed, H_2 reduction has been suggested to modify the surface morphology and the effect varies with the treatment temperature [12,13]. The possible changes in surface area after reduction and oxidation prompted us to study the effect of reduction and oxidation on surface area. A direct consequence of accurate measurements on PdO surface area is to allow for the proper measurement of turnover rates. The surface morphology of palladium oxide formed on Pd(111) and Pd(110) single crystals and the influence of H_2 reduction on the oxidized surfaces were studied by scanning

* Corresponding author. Current address: School of Chemical Engineering, Purdue University, 480 Stadium Mall Drive, West Lafayette, IN 47907-2100. Fax: (765) 494-0805.
E-mail address: fabio@purdue.edu (F.H. Ribeiro).

0021-9517/$ – see front matter
doi:10.1016/j.jcat.2004.03.035

tunnelling microscopy (STM) and temperature-programmed desorption (TPD). The surface area measurements were carried out by ^{18}O isotope exchange [14,15] and by surface area integration of STM images. We will show that after oxidation in O_2 (100 and 150 Torr) at 600 K, the surface area for both Pd(111) and Pd(110) single crystals increases by a factor of approximately two and that reduction in H_2 decreases the surface area. Thus, one should realize when working with Pd catalysts that there will be variation of surface area after oxidation and reduction treatments.

2. Experimental methods

The experiments were carried out in a specially designed system, which consisted of three chambers: ultra-high vacuum (UHV) analysis chamber, UHV STM chamber, and high-pressure reactor. The analysis chamber was equipped with X-ray photoelectron spectroscopy (XPS), Auger-electron spectroscopy (AES), low-energy electron diffraction (LEED), and TPD. The STM chamber accommodated an ambient-temperature UHV STM (RHK, Inc.). The base pressure in the UHV chambers were 5×10^{-10} Torr (1 Torr = 133.3 Pa). The high-temperature/high-pressure treatments were carried out in the high-pressure reactor (base pressure 2×10^{-8} Torr). The sample could be transferred between the chambers, without exposure to the atmosphere, by means of a 142 cm long transfer arm.

The 0.8 mm thick, 7.2 mm diameter Pd(111) and 1 mm thick, 8.5 mm diameter Pd(110) single crystals (both Princeton Scientific Corp., misalignment $< 0.5°$) were used as planar model catalysts. The temperature was measured by a chromel–alumel thermocouple spot-welded onto the side of the sample. In the analysis chamber, the sample was heated by electron-bombardment from the rear. In the reaction chamber, the sample was heated by an infrared lamp (Research, Inc.) from the front.

The temperature-programmed desorption spectra were collected at a constant heating rate of 5 K s^{-1}. The coverage was calculated by integrating the area under the TPD peak and measured in monolayers (1 monolayer = 1 ML = 1.53×10^{15} atoms cm^{-2} on Pd(111) and 0.94×10^{15} atoms cm^{-2} on Pd(110)) by comparing to standard calibration values [16,17]. STM images were obtained using Pt–Ir tips electrochemically etched in $NaCl/NaNO_3$ melt. The areas presented here are an average of at least 10 images; the variation in the area among the images is about 20%.

The crystal cleaning procedures consisted of cycles of Ar^+ sputtering at room and elevated temperatures, flashing in UHV, and exposure to O_2 and NO_2 followed by annealing at 1100 K for 60 s in UHV. The sample cleanness was checked by TPD, AES, and LEED. The NO_2 and O_2 gases were introduced into the analysis chamber through a capillary dozer.

The following experimental protocol was used for H_2 reduction experiments. The single crystal was oxidized for 30 min in 150 Torr of O_2 at 600 K and then cooled to room temperature (RT) before oxygen was pumped out. The oxidized sample was heated to the desired reduction temperature at a pressure in the reaction chamber better than 10^{-7} Torr and then 1 Torr of H_2 was introduced for 1 min. The H_2 was evacuated at a pressure better than 10^{-6} Torr before the reduced sample was cooled to RT.

The crystal structure of the oxide formed on the surface of Pd single crystals by oxidation in 150 Torr O_2 at 600 K for 30 min was checked by X-ray diffraction (XRD, Rigaku Geigerflex) with Cu-K_α radiation source and a Ni filter. The sample was dismounted from the standard STM sample holder before analysis by XRD.

The combustion of methane on Pd single crystals was performed in the 615 cm^3 batch reactor with reaction gases being introduced from a gas manifold in the following order: N_2 (624 Torr), O_2 (160 Torr), and finally CH_4 (16 Torr). The reactants were mixed for 30 min before reaction by a circulation pump Model MB-21 (Metal Bellows, Inc.) at a nominal rate of 1000 cm^3 min^{-1}. Reaction (600 K) was normally carried out for 60 min with about 2.5% of the CH_4 being consumed. The reaction mixture was analyzed with an Agilent 6890 Series gas chromatograph using a thermal conductivity detector, and a 15-ft Carboxen 1000, 60/80 mesh column.

The ^{18}O isotope exchange experiment was performed in the high-pressure reactor following the procedure described before [14]. Briefly an oxidized palladium sample was exposed to 5 Torr $^{18}O_2$ at 600 K for 12 s, and the uptake of ^{18}O exchanged was then measured by TPD analyzing all gases containing labeled oxygen.

3. Results

3.1. Surface area measurements: STM image analysis and ^{18}O isotope exchange

The surface areas were measured by STM image analysis and ^{18}O isotope exchange. The method using STM images relies on the generation of the surface topographic image by STM and therefore can be used for samples that are conductors and that can be outlined by the microscope tip. The surface area is then calculated by taking discrete image pixels and joining three contiguous points to make one triangle. Integration of the area of individual triangle gives the total area. In detail, each STM image is collected as a grid of 512×512 points. Each point (i, j) of a STM image can be described in Cartesian coordinates by $x_{i,j}$, $y_{i,j}$, $z_{i,j}$ (x, y, z projections). Three adjacent points, for instance, $(x_{i,j}\ y_{i,j}\ z_{i,j})$, $(x_{i+1,j}\ y_{i+1,j}\ z_{i+1,j})$ and $(x_{i,j+1}\ y_{i,j+1}\ z_{i,j+1})$ are used to construct a 3D oriented triangle. The total surface area is obtained by summing all triangle areas for each i and j from 1 to 512. Since other triangles can be constructed on other sets of the adjacent points, for instance $(x_{i,j}\ y_{i,j}\ z_{i,j})$, $(x_{i,j+1}\ y_{i,j+1}\ z_{i,j+1})$

and $(x_{i+1,j+1}\ y_{i+1,j+1}\ z_{i+1,j+1})$, the surface area is averaged through the possible choice of triangles. No filtering or smoothing process was applied to the STM images prior to surface area calculations.

The ^{18}O isotope exchange method is based on the detailed characterization of the ^{18}O exchange kinetics by Au-Yeung et al. [18]. The conditions described in the experimental methods section were designed to ensure that the exchange between ^{16}O in PdO and $^{18}O_2$ isotope in the gas phase would happen only on the surface, without appreciable ^{18}O diffusion to the bulk. In fact, the rate for recombination of oxygen atoms at the surface of PdO was about 4 s^{-1} at 600 K [18] and this amounts to about 50 turnovers per site in the 12 s the exchange lasts. The number of equivalent layers that oxygen atoms diffuse under exchange conditions was about 0.05 ML on both Pd(111) and Pd(110) [19]. Thus, only surface oxygen should be exchanged.

The results of the surface area measurement on palladium after oxidation in O_2 and catalytic combustion of a lean CH_4 mixture (O_2:CH_4 = 10:1) at 600 K are summarized in Table 1. It was found out that the two proposed methods: surface area integration of STM images and ^{18}O exchange agreed within ±20%. In addition, the two methods provided consistent results with the measurement of the surface area of a polycrystalline Pd foil following CH_4 combustion in lean condition [14] which is listed in the last row in Table 1.

Table 2 provides comparisons on the surface area increase after O_2 oxidation of Pd(110), Pd(111), 8.5% Pd/Al_2O_3, and 10% Pd/ZrO_2 [10]. For supported catalysts, the surface areas were determined by H_2–O_2 titration, after sample reduction. The procedure was described in detail in [10]. Briefly, metallic Pd-supported catalysts were prepared by calcination at 1123 K in air for 24 h followed by quenching to LN_2 temperature; metal is the stable phase under these conditions. The oxide phase was then prepared by treating the metallic phase at 973 K in air for 24 h. Before the surface area measurement by chemisorption, the oxide-supported catalysts were reduced in 1 atm H_2 at 373 K for 1. After oxidation, the surface area for the Pd-supported catalysts increased approximately by a factor of 2.5 (Table 2).

Table 1
Comparison of surface area determined by STM image analysis (STM) and ^{18}O isotope exchange (^{18}O)

Sample	Treatment condition	Surface area increase[a]	
		STM	^{18}O
Pd(111)	Oxidation	1.8	2.2
	Reaction	3.2	3.0
Pd(110)	Reaction	1.6	1.8
Pd foil	Reaction	–	2.2[b]

Oxidation carried out at 100 Torr O_2, 600 K, 10 min, and reaction at 600 K, 16 Torr CH_4, 160 Torr O_2, 624 Torr N_2, 60 min.

[a] Surface area increase = $\frac{\text{Oxide surface area}}{\text{Metal surface area}}$.

[b] Monteiro et al. [14].

3.2. Oxidation of Pd(111) and Pd(110) single crystals

Exposure of the Pd(111) and Pd(110) single crystals to 150 Torr of O_2 at 600 K for 30 min resulted in palladium oxide formation, which was monitored by AES and XPS (spectra not shown). The Auger peaks of oxygen were located at 490 and 510 eV, and the O/Pd atomic ratio was approximately 0.7. This value was lower than the expected value for PdO due to electron beam decomposition of the oxide, with the oxygen desorbing as O_2 [14,20]. The core-level Pd $3d_{5/2}$ peak was located at 336.8 eV, shifted 1.8 eV from the metallic peak position at 335.0 eV due to oxidation. On Pd(111) after oxidation, no X-ray diffraction pattern corresponding to PdO could be observed; only the peaks corresponding to the metal were observed. The oxygen uptakes on the Pd(111) and Pd(110) surfaces were 22 ML and 27 ML, respectively.

The STM images obtained after exposure of Pd(111) and Pd(110) single crystals to 150 Torr of O_2 at 600 K for 30 min are shown in Fig. 1. Both oxidized Pd(111) and Pd(110) single crystals showed a similar amorphous PdO surface morphology. The surface was composed of semispherical oxide agglomerates that tended to aggregate into a "cauliflower-like" structure. In general, the agglomerate size varied depending on the oxygen pressure and the exposure time. Under the reaction conditions in Fig. 1, the agglomerates grown on the Pd(111) and Pd(110) surfaces were 4.3 ± 0.7 and 3.4 ± 1.1 nm in diameter, respectively. Although the surface roughness did not allow us to draw any conclusion on preferential orientations that the oxide agglomerates grew, prior work has shown that for the Pd(111) surface, the oxide agglomerates appeared first in the vicinity of steps, whereas the $\langle 1\bar{1}0 \rangle$ direction was preferential during the early stages of Pd(110) oxidation [19].

The surface morphologies of Pd(111) and Pd(110) after methane combustion in lean condition at 600 K are presented in Fig. 2. A clearer "cauliflower-like" structure 20 ± 5 nm in size is visible on both Pd surfaces. The surface area was

Table 2
Surface area increase after oxidation of Pd catalysts

Sample	Surface area increase[a]	Oxidation condition	Method of measurement	Reference
8.5% Pd/Al_2O_3	2.7	973 K, air, 24 h	H_2–O_2 titration	[10]
10% Pd/ZrO_2	2.5	973 K, air, 24 h	H_2–O_2 titration	[10]
Pd(110)	1.9	600 K, 150 Torr O_2, 30 min	STM image analysis	Present work
Pd(111)	2.3	600 K, 150 Torr O_2, 30 min	STM image analysis	Present work

[a] Surface area increase = $\frac{\text{Oxide surface area}}{\text{Metal surface area}}$.

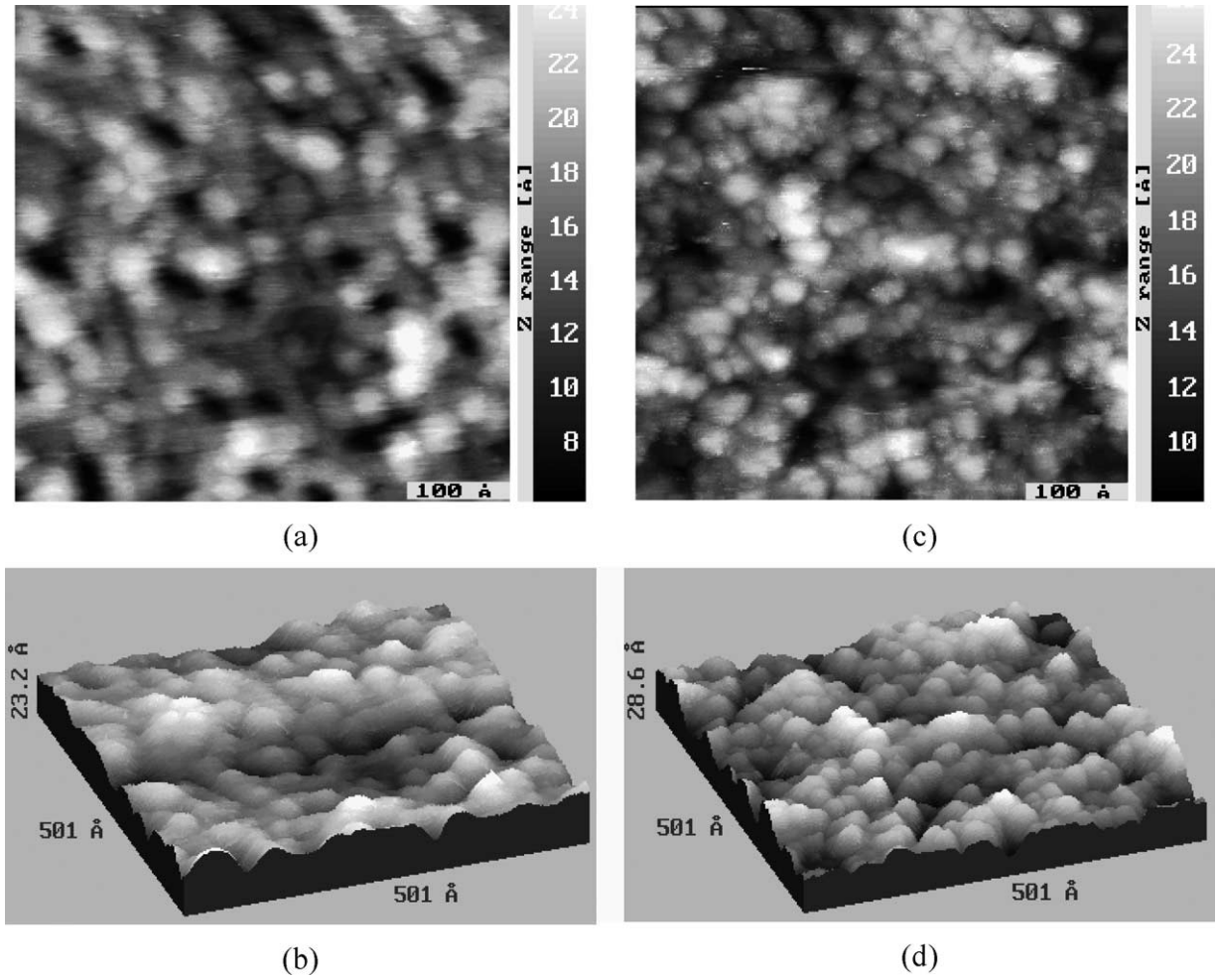

Fig. 1. STM images obtained after exposure of Pd(111) (a and b) and Pd(110) (c and d) single crystals to 150 Torr of O_2, at 600 K for 30 min. The sample bias was 1 V; the tunneling current was 0.5 nA.

higher as compared to the oxidized surface in pure O_2, particularly for the Pd(111) surface (Table 1).

3.3. H_2 reduction

To investigate the effect of H_2 reduction on surface morphology, the Pd(111) and Pd(110) surfaces preoxidized in 150 Torr of O_2 at 600 K for 30 min were studied after reduction in 1 Torr H_2 at 373 and 673 K. The lower temperature of 373 K is used for H_2–O_2 titration on supported Pd catalysts, see, for example [9,10]. The higher temperature of 673 K is used under vacuum for removing adsorbed hydrogen present on Pd after reduction and before hydrogen chemisorption [21]. According to the PdH_n phase diagram [22], no β-phase palladium hydride is expected under these reduction conditions. No oxygen was observed by TPD and by AES after the reduction at both 373 and 673 K, showing that the samples were completely reduced.

The desorption of residual hydrogen was detected by TPD from the Pd(110) surface reduced at 373 K. No LEED pattern was observed after 373 K reduction, which revealed the formation of an amorphous Pd metal overlayer. As shown by STM in Figs. 3a and 3c, the surface was rough with metal agglomerates visible. The agglomerates were not of spherical shape as before reduction (see Fig. 1), but elongated with an aspect ratio around 2–2.5:1 (4.5 ± 0.5 nm vs 2.1 ± 0.4 nm on Pd(110) and 3.5 ± 0.7 nm vs 1.6 ± 0.4 nm on Pd(111)). On the Pd(111) surface, the agglomerates were slightly angled with respect to the monoatomic steps, which were barely distinguishable. On the Pd(110) surface, the "rod-shaped" agglomerates were aligned along $\langle 1\bar{1}0 \rangle$.

Temperature-programmed desorption did not reveal any hydrogen desorption after reduction at 673 K. A diffuse (1×1) pattern referred to the bare unreconstructed surface was observed by LEED for both Pd(111) and Pd(110) surfaces. The surface reduced at 673 K was smoother than that after 373 K reduction as shown in Figs. 3b and 3d with monoatomic steps visible on the Pd(111) surface. One noticeable difference was that the step was curved and not straight as on a clean Pd(111) surface. Several holes with mean size of 3 nm and monoatomic depth did not heal on the terraces. A mesoscopic ordered island structure composed of

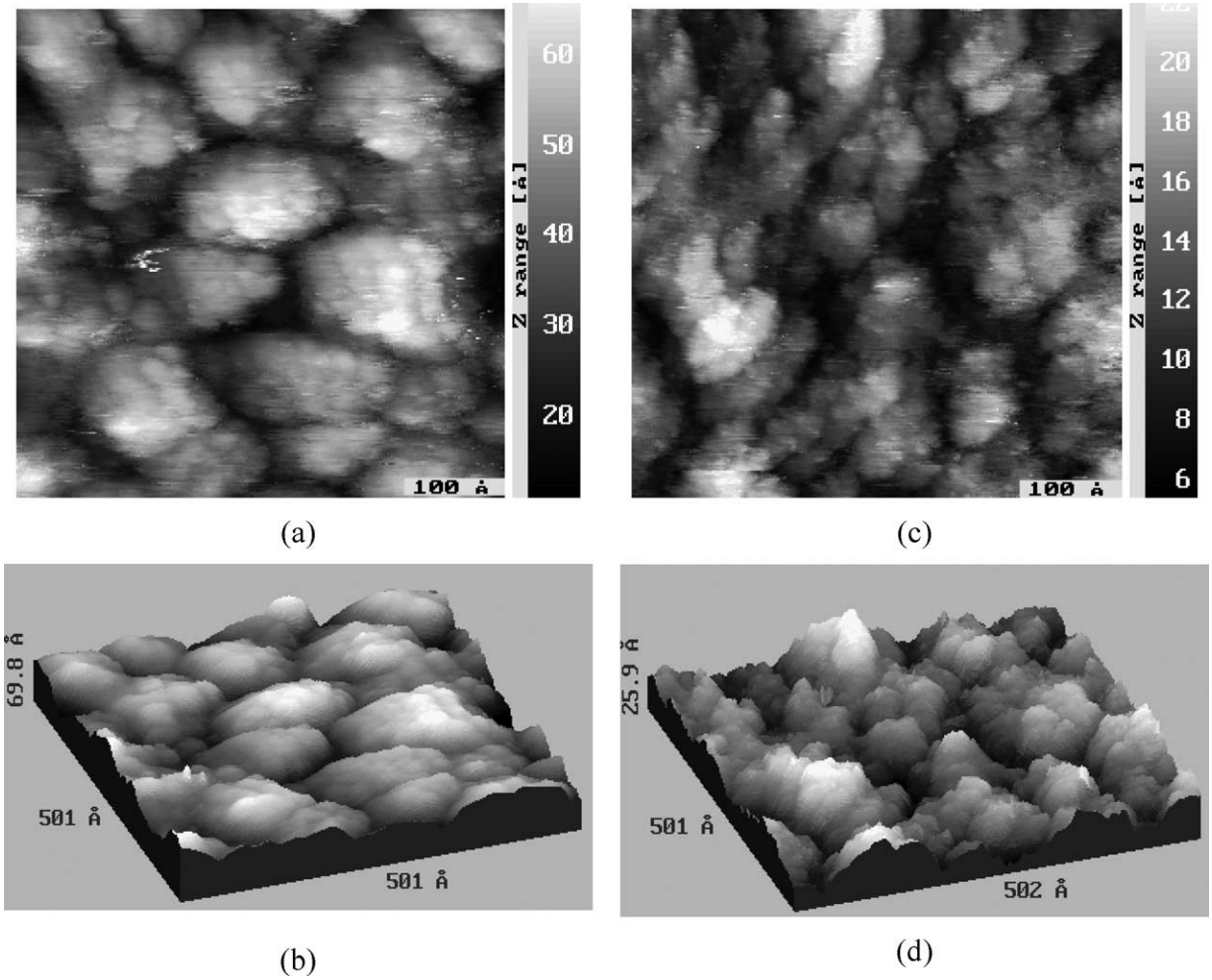

Fig. 2. STM images obtained from Pd(111) (a and b) and Pd(110) (c and d) surfaces exposed to 16 Torr CH_4, 160 Torr O_2, and 624 Torr N_2 at 600 K for 60 min. The sample bias was 1 V; the tunneling current was 0.5 nA.

alternating bright and dark islands appeared on the Pd(110) surface after H_2 reduction at 673 K. The mean size of the island was approximately 14 nm in the ⟨100⟩ direction and 20 nm in the $\langle 1\bar{1}0\rangle$ direction. The height difference between the islands was 0.14 nm, which is equal to the height of the monoatomic step on the Pd(110) surface. Each mesoscopic island was composed of elongated agglomerates with aspect ratio of 3–4:1 (6.9 ± 1.1 nm vs 2.2 ± 0.6 nm).

The surface area decrease after H_2 reduction is summarized in Table 3. It is shown that the surface area of the preoxidized Pd(111) and Pd(110) single crystals decreased even after reduction at 373 K, and the effect was more pronounced after 673 K reduction.

Table 3
Surface area decrease after reduction of preoxidized Pd(111) and Pd(110) evaluated by integration of STM images

Oxidized sample	H_2 reduction temperature	Surface area increase factor[a]
Pd(110)	No reduction	1.9
	373 K	1.5
	673 K	1.1
Pd(111)	No reduction	2.3
	373 K	1.3
	673 K	1.1

Oxidation conditions were 150 Torr O_2 at 600 K for 30 min. Reduction conditions were 1 Torr H_2 at 373 or 673 K for 1 min.

[a] Surface area increase factor $= \frac{\text{Oxide surface area}}{\text{Metal surface area}}$.

4. Discussion

4.1. STM image analysis and ^{18}O isotope exchange

We report the surface area integration of STM images and ^{18}O isotope exchange as methods to measure the surface area on palladium single crystals after O_2 oxidation, CH_4 combustion, and H_2 reduction. In the method of ^{18}O isotope exchange, the exchange conditions between ^{18}O in the gas phase and ^{16}O in PdO should be chosen to ensure enough exchange turnovers and to limit bulk diffusion.

In certain circumstances, experimental errors also exist in the STM image analysis method. At low bias voltages STM probes the oxide–substrate interface, whereas STM be-

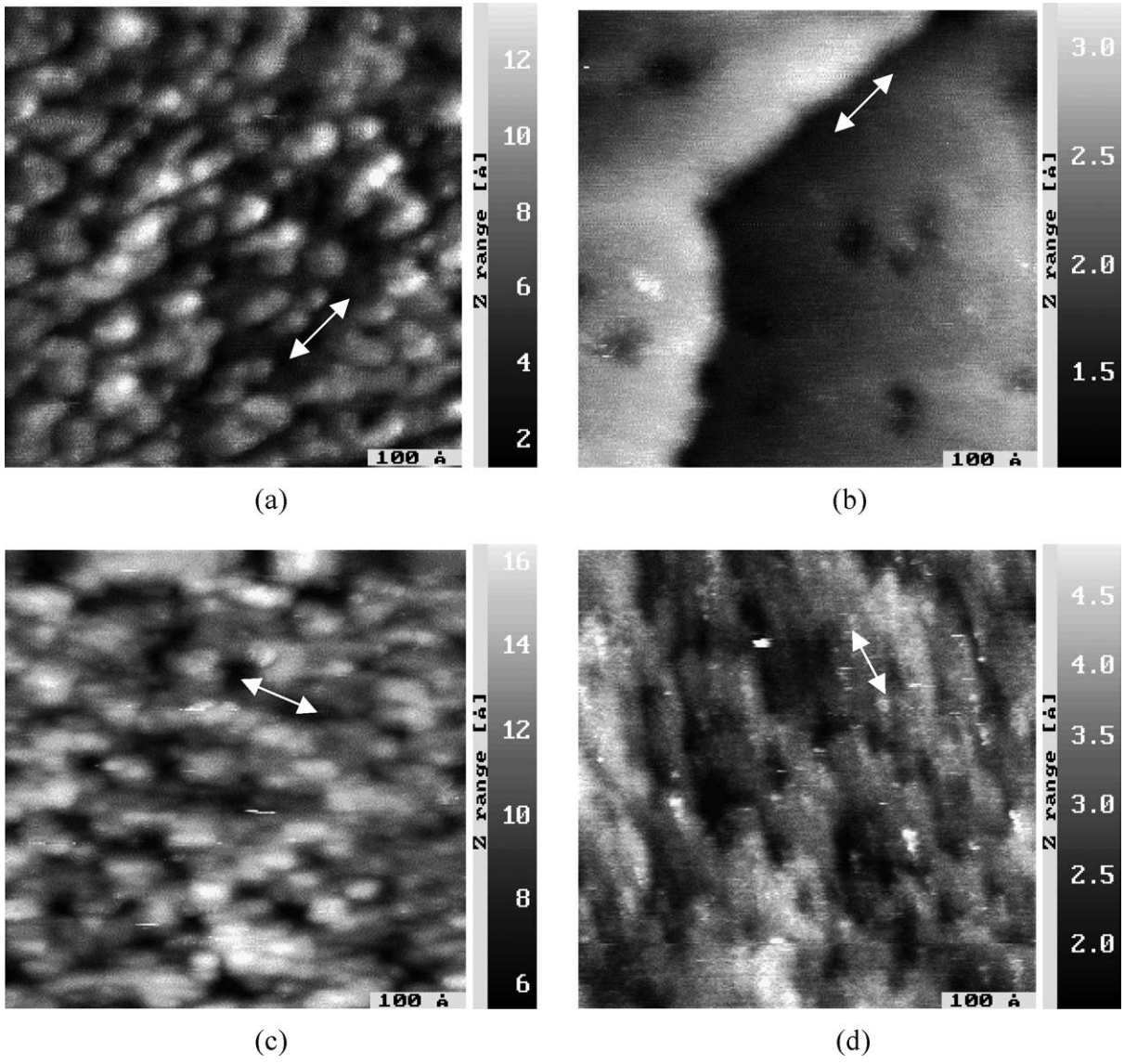

Fig. 3. STM images obtained after reduction in 1 Torr of H_2 of the preoxidized Pd(111) (a and b) and Pd(110) (c and d) surfaces at 373 K (a, c) and at 673 K (b, d). Arrows designate the step orientation in (a and b), and $\langle 1\bar{1}0 \rangle$ in (c and d). The sample bias was 1 V; the tunneling current was 0.5 nA.

comes more sensitive to the vacuum–oxide interface at high bias voltage. This effect was demonstrated for instance by Bertrams et al. [23] for a thin Al_2O_3 film on NiAl(110). No change of the tip height was detected when moving between an Al_2O_3 island and the NiAl substrate at bias voltage below 4 V (the band gap of Al_2O_3 is approximately 7–8 V). On the other hand, an apparent height of 3.5 Å with respect to the metal support was observed after the bias voltage was increased above 4 V. Hagendorf et al. [24] showed that CoO(001) islands on the Ag(001) surface appeared to be depressed at the bias voltage between −1.5 and +2.2 V, whereas above and below these voltages the islands were protruding from the substrate. The maximum height variation was 6 Å. In our experiments this effect was not significant. The variation of the size and height of the oxide clusters was in the range of 0.1–0.3 Å when the bias voltage was changed from 0.1 to 5.0 V. The thickness of the oxide layers is estimated to be in the range of 5–20 ML; and the band gap for bulk PdO is reported to be 4.0–5.0 V [25]. The absence of the "bias-voltage" dependence could be explained by the high surface conductivity of oxygen vacancies generated under UHV conditions.

The tip effect can also introduce experimental errors. In fact, the image of an object on the surface might be just tip shape deconvolution. The agglomerates might appear larger in the STM image. No changes of the surface topology and of the surface area were observed when the tip was changed, thus implying that this effect was not significant. On the other hand, if the tip cannot follow the contour of the surface, the measured surface area by STM will be in error. The good agreement between the STM data and the ^{18}O exchange data (Table 1) allows us to rule out this effect as well.

Another important issue is the dependence of the surface area calculated from a STM image as a function of the grid

step as discussed by Brown et al. [26]. The $x-y$ step used in our study was approximately 1 Å (500 × 500 Å with image resolution 512 × 512 lines), two times smaller than the Pd–O bond length (2.02 Å). The proper choice of the grid step is supported by the comparison with the ^{18}O isotope exchange method as shown in Table 1.

4.2. Oxidation of Pd single crystals

Oxidation of Pd single crystals in low pressure (< 1 Torr, typically $< 10^{-6}$ Torr) O_2 has been studied previously, see, for example [16,17,20,27–37]. Chemisorption of oxygen atoms on Pd single crystals results in a $p(2 \times 2)$ overlayer with 0.25 ML coverage on Pd(111) [16,38], $p(2 \times 2)$ and $c(2 \times 2)$ overlayers on Pd(100) with 0.25 and 0.5 ML coverages, and the reconstructed $c(2 \times 4)$ superstructure on Pd(110) with 0.5 ML coverage [17]. The oxygen uptake beyond the saturation coverage could be reached (2.3 ML on Pd(111), 0.8 ML on Pd(100), and 1.8 ML on Pd(110)) by dosing stronger oxidants such as NO_2 [16,27,30] or exposing to O_2 at high pressures and temperatures [17,20,29]. A surface oxide appears on Pd(111) [16,20] and Pd(110) [32,39], which presents a complex crystal structure distinct from that of PdO or the original metallic facets. On Pd(100), the surface oxide appears to have a structure close to PdO(001). It is suggested that PdO forms through a nucleation mechanism [16]. Once the bulk oxide forms, the surface roughens [16,27].

It is possible that bulk palladium oxide could be formed only when a critical concentration of dissolved oxygen was reached in the near-surface region. The formation of this stoichiometric PdO was characterized by the drastically dropped oxygen uptake rate, the complete fading of the metallic Pd(110) LEED pattern, the 0.2–0.7 O/Pd atomic ratio detected by AES, and the roughened cauliflower-like surface structure imaged by STM [19]. The roughened surface structure with an increase in surface area could be rationalized as a major lattice expansion during the chemical transformation 'Pd metal' → 'Pd oxide'. The Pd atom density for the oxide is only 60% of the density for the metal structure. In addition, the Pd–Pd nearest neighbor distance is 3.04 Å for PdO, about 10% larger than the 2.75 Å for Pd metal.

The fact that we did not observe any XRD pattern of PdO, which should be detectable for the thick PdO layer (2–7 nm estimated from STM images), is an indication that the oxide layer is either amorphous or crystalline with crystallites too small to diffract coherently. The STM images do not reveal preferential growth and thus we conclude that the oxide layer is amorphous. A number of semispherical oxide agglomerates were observed in this study (Fig. 1) possibly due to many nucleation sites of oxide growth. Unfortunately we do not know the nature of these sites. It might be structural defects but most probably this is a fluctuation of the oxygen concentration in the near-surface region, which causes a local transformation Pd → PdO. The mean size of the oxide agglomerates is different on the Pd(111) and Pd(110) surfaces. The most dense Pd(111) surface expanded more than the more open Pd(110) surface. The concentration of dissolved oxygen also might affect the oxide agglomerate size. Oxidation of Pd single crystals including Pd(111), Pd(100) and Pd(110) suggested that the oxygen diffusion from surface to the bulk depends on the surface crystallography with the highest rate of diffusion determined on the open Pd(110) surface. Indeed, the oxygen uptakes were 13 ML, 17 ML, and 25 ML on Pd(111), Pd(100), and Pd(110) respectively after exposure to 25 Torr O_2 at 600 K for 10 min [19]. Therefore the Pd → PdO transformation might proceed at a higher bulk oxygen concentration for a given O_2 gas pressure for the Pd(110) single crystal, resulting in a greater number of nucleation sites. This should lead to smaller agglomerates.

It is interesting to note that the surface area increase after oxidation of a well-annealed metallic supported catalyst agrees with the corresponding result on single crystals (Table 2). This is to be expected as metal crystallites on a supported catalyst are composed of low index planes, as shown for example by TEM [40]. Thus, the increase in surface area observed on supported Pd catalysts after oxidation is caused by surface roughening.

4.3. H_2 reduction

The measurement of surface area for supported Pd catalysts requires reduction of the oxidized sample, usually in H_2, before chemisorption. Reduction in H_2, however, results in changes of the surface area as demonstrated in Table 3. Note that the reduction temperature is an important parameter. Scanning tunnelling microscopy images of the preoxidized Pd(111) and Pd(110) surfaces reduced at a temperature of 673 K demonstrated a fairly smooth surface with clearly visible monoatomic steps (Fig. 3). The surface area after reduction was only about 1.1 times higher than the metal surface area compared to the twofold increase after preoxidation. On a supported catalyst, reduction at high temperatures might also cause Pd sintering. Suh and Park [41] using transmission electron microscopy (TEM) observed significant sintering of finely dispersed Pd/C catalyst following treatment at 673 K. Logan et al. [13] detected only Rh metal agglomerates with well-defined low index facets after reduction in H_2 at 773 K. At 373 K however, the rate of reduction, i.e., the rate of generation of free Pd atoms exceeds the rate of their diffusion and recrystallization and therefore the surface remains amorphous. TEM studies by Datye et al. [12] reported the formation of an amorphous Rh metallic layer on crystalline RhO agglomerates during reduction at 323 K in hydrogen. The surface area decreased even after 373 K reduction but it could be due to the collapse of the Pd agglomerates after the PdO → Pd transformation. It is reasonable to assume that the large agglomerates should experience greater shrinking due to the bigger contribution of bulk atoms compared to surface atoms. Thus, the big-

ger agglomerates collapse more. This might explain why the oxidized Pd(110) surface showed only 24% surface area decrease after H_2 reduction at 373 K, whereas the surface area decreased 42% for oxidized Pd(111).

The main conclusion from the H_2 reduction experiments is that the area of the reduced sample is different from the area of the actual oxidized catalyst.

5. Summary

Planar model catalysts Pd(111) and Pd(110) were used to study palladium oxidation and methane combustion. The surfaces were studied by STM, TPD, XPS, AES, and LEED. The advantages of using a model catalyst approach were demonstrated by accurate surface area measurements, which were performed by the surface area integration of STM images and by ^{18}O isotope exchange. The surface area integration of STM images was performed by triangulation of the STM image based on the x/y grid with a 1 Å step. Surface ^{16}O atoms were exchanged by ^{18}O atoms in gas phase during ^{18}O exchange experiments, and the uptake was then measured by TPD. The area measurement by ^{18}O isotope exchange and by STM image analysis showed similar values.

Exposure of the Pd(111) and Pd(110) single crystals to 100–150 Torr O_2 at 600 K led to an increase in surface area by a factor of approximately two. The effect was more pronounced for the Pd(111) surface. This might be because the close packed Pd(111) surface experienced a greater lattice expansion during the Pd $\rightarrow$ PdO transformation than the open Pd(110) surface. The other explanation is that because of the higher oxidation rate on the (110) surface, smaller oxide agglomerates were formed due to a higher density of oxide nuclei. The smaller oxide agglomerates on the (110) surface created a lower surface area than the bigger agglomerates in the case of the Pd(111) surface. On both surfaces, oxide agglomerates formed an amorphous structure. A surface with more pronounced cauliflower-like structure was observed after treatment of the Pd single crystals in a lean $O_2 + CH_4$ reaction mixture.

The H_2 reduction of preoxidized Pd(111) and Pd(110) crystals resulted in the decrease of surface area of the oxidized Pd(111) and Pd(110) crystals. An amorphous metallic surface was found after reduction at 373 K, whereas an almost smooth surface with area of only 1.1 times that of clean metallic surface was observed after 673 K hydrogen reduction. Characteristic single crystal features were observed by LEED after 673 K reduction in H_2.

In conclusion, the surface area of Pd(111) and Pd(110) single crystals changes after they are subjected to O_2 oxidation, methane combustion, or H_2 reduction. The surface area change after oxidation on single crystals agrees with the ones on supported catalysts and it us due to roughening of the PdO surface. These results imply that pretreatments before Pd surface area measurement can modify the Pd surface area on supported catalysts.

Acknowledgment

We gratefully acknowledge support from the Office of Basic Energy Sciences, Chemical Sciences, U.S. Department of Energy, Grant DE-FG02-00ER15408.

References

[1] M. Boudart, G. Djega-Mariadasson, in: Kinetics of Heterogeneous Catalytic Reactions, Princeton University Press, Princeton, 1984, p. 7.
[2] M. Boudart, Chem. Rev. 95 (1995) 661.
[3] F.H. Ribeiro, A.E.S. Von Wittenau, C.H. Bartholomew, G.A. Somorjai, Catal. Rev. 39 (1997) 49.
[4] J.E. Benson, H.S. Hwang, M. Boudart, J. Catal. 30 (1973) 146.
[5] R.B. Anderson, K.C. Stein, J.J. Feenan, L.J.E. Hofer, Ind. Eng. Chem. 53 (1961) 809.
[6] C. Mallika, O.M. Sreedharan, J.B. Gnanamoorthy, J. Less-Common Met. 95 (1983) 213.
[7] W.E. Bell, R.E. Inyard, M. Tagami, J. Phys. Chem. 70 (1966) 3735.
[8] G. Bayer, H.G. Wiedemann, Thermochim. Acta 11 (1975) 79.
[9] K.-I. Fujimoto, F.H. Ribeiro, M. Avalos-Borja, E. Iglesia, J. Catal. 179 (1998) 431.
[10] F.H. Ribeiro, M. Chow, R.A.D. Betta, J. Catal. 146 (1994) 537.
[11] G. Prelazzi, M. Cerboni, G. Leofanti, J. Catal. 181 (1999) 73.
[12] A.K. Datye, Top. Catal. 13 (2000) 131.
[13] A.D. Logan, K. Sharoudi, A.K. Datye, J. Phys. Chem. 95 (1991) 5568.
[14] R.S. Monteiro, D. Zemlyanov, J.M. Storey, F.H. Ribeiro, J. Catal. 199 (2001) 291.
[15] R.S. Monteiro, D. Zemlyanov, J.M. Storey, F.H. Ribeiro, J. Catal. 201 (2001) 37.
[16] G. Zheng, E.I. Altman, Surf. Sci. 462 (2000) 151.
[17] J.W. He, P.R. Norton, Surf. Sci. 204 (1988) 26.
[18] J. Au-Yeung, A.T. Bell, E. Iglesia, J. Catal. 185 (1999) 213.
[19] J. Han, D. Zemlyanov, G. Zhu, F.H. Ribeiro, in preparation.
[20] E.H. Voogt, A.J.M. Mens, O.L.J. Gijzeman, J.W. Geus, Surf. Sci. 373 (1997) 210.
[21] P.C. Aben, J. Catal. 10 (1968) 224.
[22] J. Shu, B.P.A. Grandjean, A. Van Neste, S. Kaliaguine, Can. J. Chem. Eng. 69 (1991) 1036.
[23] T. Bertrams, A. Brodde, H. Neddermeyer, J. Vac. Sci. Technol. B 12 (1994) 2122.
[24] C. Hagendorf, R. Shantyr, K. Meinel, K.M. Schindler, H. Neddermeyer, Surf. Sci. 532–535 (2003) 346.
[25] C.Q. Sun, Surf. Rev. Lett. 7 (2000) 347.
[26] C.A. Brown, P.D. Charles, W.A. Johnsen, S. Chesters, Wear 161 (1993) 61.
[27] G. Zheng, E.I. Altman, Surf. Sci. 504 (2002) 253.
[28] E. Lundgren, G. Kresse, C. Klein, M. Borg, J.N. Andersen, M. De Santis, Y. Gauthier, C. Konvicka, M. Schmid, P. Varga, Phys. Rev. Lett. 88 (2002) 246103/1.
[29] B. Klotzer, K. Hayek, C. Konvicka, E. Lundgren, P. Varga, Surf. Sci. 482–485 (2001) 237.
[30] B.A. Banse, B.E. Koel, Surf. Sci. 232 (1990) 275.
[31] H. Niehhus, C. Achete, Surf. Sci. 369 (1996) 9.
[32] M. Nishijima, M. Jo, Y. Kuwahara, M. Onchi, Solid State Commun. 60 (1986) 257.
[33] F.P. Leisenberger, G. Koller, M. Sock, S. Surnev, M.G. Ramsey, F.P. Netzer, B. Klotzer, K. Hayek, Surf. Sci. 445 (2000) 380.
[34] D.T. Vu, K.A.R. Mitchell, O.L. Warren, P.A. Thiel, Surf. Sci. 318 (1994) 129.

[35] T.W. Orent, S.D. Bader, Surf. Sci. 115 (1982) 323.
[36] V.A. Bondzie, P. Kleban, D.J. Dwyer, Surf. Sci. 347 (1996) 319.
[37] J. Goschnick, M. Wolf, M. Grunze, W.N. Unertl, J.H. Block, J. Loboda-Cackovic, Surf. Sci. 178 (1986) 831.
[38] H. Conrad, G. Ertl, J. Kueppers, E.E. Latta, Surf. Sci. 65 (1977) 245.
[39] G. Ertl, P. Rau, Surf. Sci. 15 (1969) 443.
[40] A.K. Datye, J. Catal. 216 (2003) 144.
[41] D.J. Suh, T.-J. Park, J. Catal. 149 (1994) 486.